Apoptosis in retinal degeneration involves cross-talk between apoptosis-inducing factor (AIF) and caspase-12 and is blocked by calpain inhibitors

Daniela Sanges*, Antonella Comitato*, Roberta Tammaro*, and Valeria Marigo*†‡

*Telethon Institute of Genetics and Medicine (TIGEM), 80131 Naples, Italy; and †Department of Biomedical Sciences, University of Modena and Reggio Emilia, 41100 Modena, Italy

Edited by Jeremy Nathans, The Johns Hopkins University School of Medicine, Baltimore, MD, and approved September 21, 2006 (received for review July 24, 2006)

Molecular mechanisms underlying apoptosis in retinitis pigmentosa, as in other neurodegenerative diseases, are still elusive, and this fact hampers the development of a cure for this blinding disease. We show that two apoptotic pathways, one from the mitochondrion and one from the endoplasmic reticulum, are co-activated during the degenerative process in an animal model of retinitis pigmentosa, the *rd1* mouse. We found that both AIF and caspase-12 translocate to the nucleus of dying photoreceptors *in vivo* and in an *in vitro* cellular model. Translocation of both apoptotic factors depends on changes in intracellular calcium homeostasis and on calpain activity. Knockdown experiments defined that AIF plays the major role in this apoptotic event, whereas caspase-12 has a reinforcing effect. This study provides a link between two executor caspase-independent apoptotic pathways involving mitochondrion and endoplasmic reticulum in a degenerating neuron.

rd1 mouse | photoreceptor | retinal stem cells

Retinitis pigmentosa (RP) is a form of retinal degeneration resulting from rod photoreceptor cell death and leading to blindness. Despite the remarkable genetic heterogeneity of this disease, photoreceptors undergo a common mode of cell death: apoptosis. An autosomal recessive form of RP is caused by mutations in the rod-specific β-catalytic subunit of the phosphodiesterase gene *PDE6B* (1). The naturally occurring retinal degeneration (*rd1*) mouse is the animal model for this type of RP (2). The *rd1* mouse has elevated levels of cGMP (3, 4), and this elevation results in elevated intracellular calcium (5). Ca^{2+} concentration within the cytosol as well as Ca^{2+} tides and ebbs within various organelles, such as mitochondria, nucleus, and endoplasmic reticulum (ER), are important in regulating many cellular functions such as neuronal survival or cell death.

There are instances, most notably after Ca^{2+} overload, in which the cell-death pathway elicited differs from classical caspase-mediated apoptosis. Calpains are cysteine proteases activated by calcium during apoptotic processes (6). Calpain I and II (μ- and *m*-calpain) are expressed in the retina (7), and recent reports showed activation of calpain and cathepsin D in *rd1* mice (5, 8). Several proteins are known targets of calpain protease activity, such as caspase-12 and apoptosis-inducing factor (AIF). Caspase-12, localized to the ER (9), can be activated by *m*-calpain in the presence of the pancaspase inhibitor zVAD.fmk (10). Interestingly, caspase-12 has been linked to neuronal degeneration in neurotoxicity caused by amyloid-β protein (9), by prion protein (11), and in animal models of ALS (12). The cleaved active form of caspase-12 participates to the apoptotic event by translocation to the nucleus (13); however, it is unclear whether caspase-12 can induce chromatin fragmentation. AIF also directly translocates to the nucleus to execute DNA fragmentation that culminates in cell death (14). The translocation of AIF from mitochondria to the nucleus has been implicated in neuronal demise and in photoreceptor cell death after retinal detachment (15–17). Cleavage and release of AIF from mitochondria is regulated by μ-calpain (18) and can occur independently from cytochrome *c* release (19).

In this study, we demonstrate a direct correlation of increased intracellular Ca^{2+}, calpain activation, and nuclear translocation of AIF and caspase-12 in apoptotic photoreceptors. We also show that AIF plays the key role in apoptosis activation. Finally, we provide evidences that treatment with calpain inhibitors is able to block activation of AIF and caspase-12 and, consequently, apoptosis *in vitro* and *in vivo*.

Results

AIF and Caspase-12 Are Activated During Apoptosis in *rd1* Retinas. To investigate which apoptotic pathway is activated during the degenerative process in *rd1* retinas, we analyzed changes in subcellular localization of two factors involved in intrinsic apoptotic signals, AIF and caspase-12. Based on our analysis of apoptosis progression and on other reports (20), we chose P11 for all our studies. At this stage, rods are undergoing apoptosis, followed then by cones not expressing *Pde6b* (21). AIF is a mitochondrial protein mostly localized in the inner segment of photoreceptor cells containing mitochondria and ER and in the cytoplasm of other retinal cells (Fig. 1*A*; and see Fig. 6*A*, which is published as supporting information on the PNAS web site). In *rd1* retinas, AIF could be detected in some photoreceptor nuclei and colocalized with TUNEL that labels chromatin fragmentation in cells undergoing apoptosis (Figs. 1 *E–H* and 6*B*). Similarly, in wild-type (wt) mice, caspase-12 is preferentially found in the inner segment containing the ER of photoreceptor cells (Figs. 1*B* and 6*C*). Double labeling with TUNEL showed caspase-12 in the nucleus of *rd1* cells undergoing apoptosis (Figs. 1 *F–H* and 6*D*). Interestingly, we found that all nuclei containing activated AIF also contained activated caspase-12. We calculated that 80% of the cells in apoptosis also showed nuclear staining for AIF and caspase-12 (Fig. 1*M*). This same analysis was performed also at postnatal day (P)10 and P13, and we calculated similar percentages of AIF- and caspase-12-positive nuclei (data not shown), suggesting that lack of detection of AIF and caspase-12 in 20% of apoptotic photoreceptors is not because of the time chosen for our analysis. Western blot analysis confirmed nuclear localization of AIF and activated caspase-12 fragments in *rd1* and not in the wt retinas (Fig. 1*N*). No activated caspase-3 or caspase-9 were detectable in cytosol extracts from wt and *rd1* retinas (data not shown), as expected from other reports (22, 23). Translocation of AIF and caspase-12 appeared specific; in

Author contributions: V.M. designed research; and D.S., A.C., and R.T. performed research.

The authors declare no conflict of interest.

This article is a PNAS direct submission.

Abbreviations: AIF, apoptosis-inducing factor; ER, endoplasmic reticulum; P, postnatal day; RP, retinitis pigmentosa; shRNA, short hairpin RNA; wt, wild type.

‡To whom correspondence should be addressed at: Telethon Institute of Genetics and Medicine (TIGEM), Via P. Castellino 111, 80131 Naples, Italy. E-mail: marigo@tigem.it.

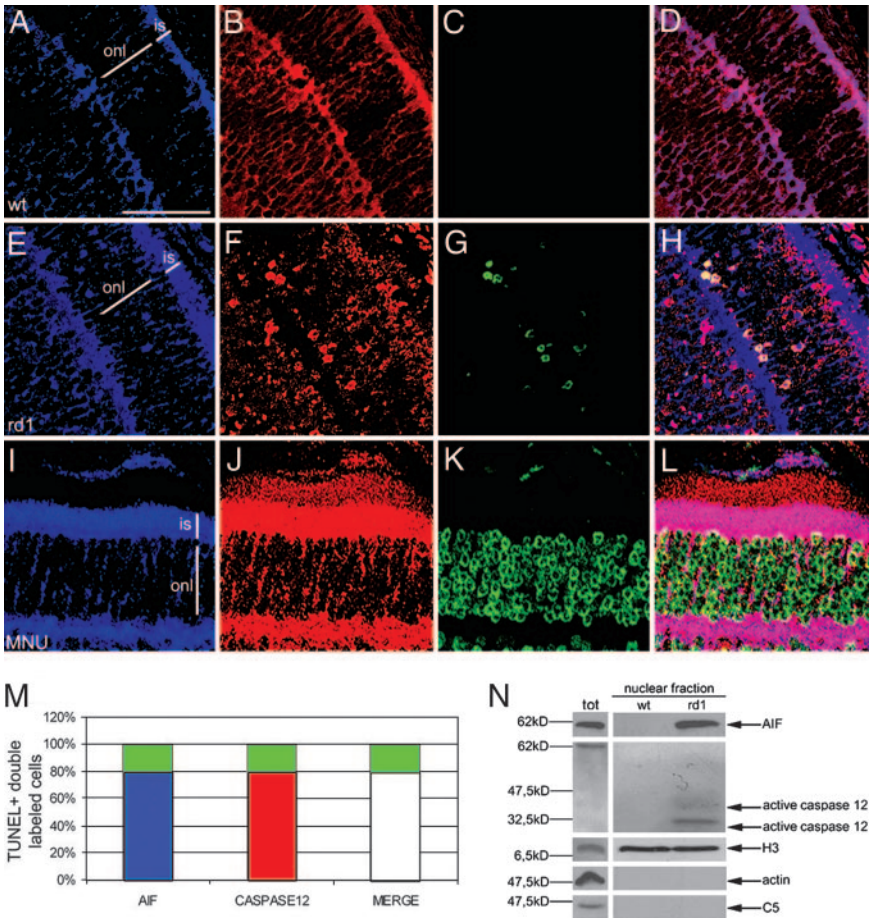

Fig. 1. Translocation of AIF and caspase-12 in apoptotic photoreceptor nuclei of *rd1* retina. (*A–L*) Confocal microscopy of P11 retinal sections triple stained with antibodies anti-AIF (blue) or anti-caspase-12 (red) and TUNEL (green). Merged images are shown in *D*, *H*, and *L*, where white indicates triple labeling. is, inner segment; onl, outer nuclear layer. (Scale bar, 100 μm.) (*M*) Percentage of AIF-labeled (blue), caspase-12-labeled (red), and double-labeled (white) apoptotic nuclei (green) in *rd1* mice. (*N*) Western blot of nuclear-enriched lysates purified from P11 wild-type (wt) and *rd1* retinas. Western blot was normalized with nuclear marker histone H3 (H3). Contaminations from mitochondria and cytosol were evaluated by analysis of a mitochondrial protein (C5) and β-actin. Inactive form of caspase-12 is shown in Western blot from total extract (tot, first lane).

fact, no changes in subcellular localizations of mitochondrial cytochrome *c* and ER marker ERAB were observed in *rd1* photoreceptors (Fig. 6 *E–H*).

Finally, we treated wt mice with nitrosomethyl-urea, causing massive and fast apoptosis in the retina. In these conditions, almost all photoreceptor nuclei were TUNEL-positive, but none of them showed nuclear localization of either AIF or caspase-12 (Fig. 1 *I–L*), demonstrating that their translocation was specific to the genetic pathological condition.

***In Vitro* Analysis of AIF and Caspase-12 Activation in *rd1* Photoreceptors.** To better characterize, at a molecular level, colocalization of AIF and caspase-12 and the cells undergoing apoptosis, we took advantage of an *in vitro* system to differentiate photoreceptor cells. Neurospheres, derived from the adult ciliary margin were *in vitro*-differentiated to the various retinal neuronal cell types (24). Photoreceptors were characterized by expression of three different markers (rhodopsin, Pde6β, and cGMP-gated channel Cnga). Approximately 40% of the wt cells in culture expressed the three photoreceptor-specific proteins, whereas cells derived from *rd1* mice expressed rhodopsin and Cnga, but not Pde6β, as expected (Fig. 2 *A–E*, *G*, *H*, *J*, and *K*). Interestingly, we found that only *rd1*-differentiated cells were undergoing apoptosis *in vitro* (Fig. 2 *F*, *I*, and *L*). All apoptotic cells were also expressing photoreceptor markers, and apoptosis was never observed in cells labeled with markers for amacrine and bipolar and horizontal retinal neurons (Fig. 2 *M–O*).

Subcellular localizations of AIF and caspase-12 were analyzed in wt and *rd1* photoreceptors *in vitro*. In these experiments, cells were treated with retinoic acid to achieve a faster and higher rod differentiation. Both AIF and caspase-12 localized inside the apoptotic nuclei of *rd1* cells (Fig. 3 *E–H*, arrows) differently from wt cells (Fig. 3 *A–D*). As shown *in vivo*, also in *in vitro*-differentiated photoreceptors AIF and caspase-12 colocalized in the apoptotic nuclei (Fig. 3*H*, arrows). We also analyzed cytochrome *c* localization, and we did not detect mitochondrial release of cytochrome *c* during photoreceptor apoptosis (Fig. 3 *I* and *J*). This finding confirmed the specificity of translocation of AIF not affecting other mitochondrial molecules, and this was true also for caspase-12 as analyzed with an ER-localized protein (ERAB) (Fig. 3 *K* and *L*). Finally, to define whether activation of AIF and caspase-12 was correlated to changes in intracellular Ca^{2+} concentration, we compared Ca^{2+} content between wt and *rd1* in *in vitro*-differentiated photoreceptors. A progressive increase in Ca^{2+} concentration was detected in *rd1* cells during differentiation (Fig. 3 *M–O*). We measured the enhancement in intracellular Ca^{2+} levels in *rd1* cells of three times after 11 days in culture, and treatment with *cis*-diltiazem, a calcium blocker, prevented calcium increase (Fig. 3*O*). Finally, by treatment of wt *in vitro*-differentiated photoreceptors with thapsigargin, which inhibits ER-associated Ca^{2+}-ATPase

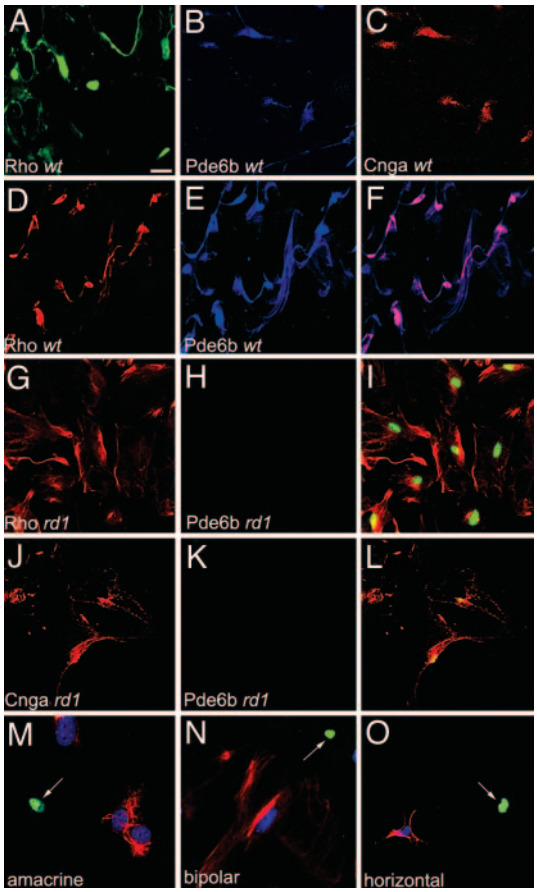

Fig. 2. Apoptosis in *in vitro*-differentiated *rd1* photoreceptors. (*A–C*) *In vitro*-differentiated photoreceptors derived from wt retinas stained with antibodies anti-rhodopsin (Rho, green), anti-phosphodiesterase6β (Pde6b, blue), and anti-rod cGMP-gated ion channel α-subunit (Cnga, red). wt cells express the three rod-specific markers. (Scale bar, 20 μm.) (*D–L*) wt (*D–F*) and *rd1* (*G–L*) differentiated photoreceptors were triple stained with anti-rhodopsin (red), anti-Pde6b (blue), anti-Cnga (red), and TUNEL (green). Merged images are shown in *F*, *I*, and *L*. (*M–O*) *In vitro*-differentiated *rd1* retinal cells were double stained with TUNEL (green) and antibodies for the amacrine cell marker syntaxin (*M*), the bipolar cell marker Pkcα (*N*), or the horizontal cell marker calbindin (*O*). Nuclei were stained with DAPI (blue). Cells that undergo apoptosis (arrows) do not express markers of amacrine, bipolar, and horizontal retinal cells. (Scale bar, 10 μm.)

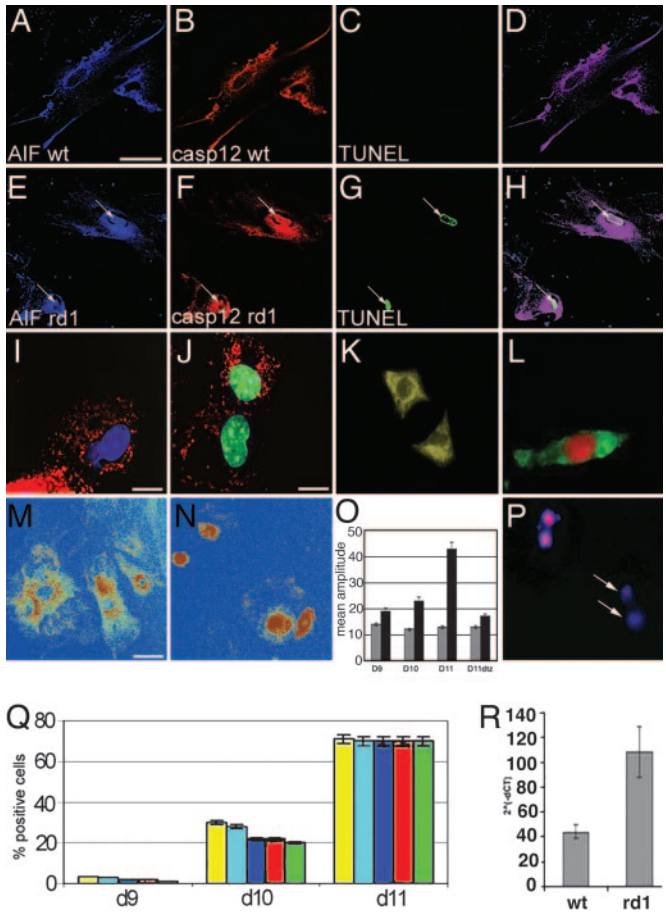

Fig. 3. Correlation among Ca^{2+} levels, calpain activation, and AIF and caspase-12 nuclear translocation in *rd1* apoptotic cells. (*A–H*) Differentiated retinal cells from wt (*A–D*) and *rd1* (*E–H*) mice triple stained with anti-AIF (blue), anti-caspase-12 (red), and TUNEL (green). Merged images are shown in *D* and *H*. AIF and caspase-12 in *rd1* TUNEL-positive cells are detected inside the nuclei (arrows in *E–H*). (Scale bar, 10 μm.) (*I* and *J*) wt (*I*) and *rd1* (*J*) *in vitro*-differentiated retinal cells double stained with anti-cytochrome *c* (red) and TUNEL (green). Nuclei were counterstained with DAPI (blue). (Scale bar, 2 μm.) (*K* and *L*) wt (*K*) and *rd1* (*L*) *in vitro*-differentiated retinal cells were double stained with anti-caspase-12 (red) and anti-ERAB (green). (*M* and *N*) Pseudocolored images analyzing intracellular Ca^{2+} distribution in wt (*M*) and *rd1*-differentiated (*N*) retinal cells. Brown represents high Ca^{2+}, and blue represents low Ca^{2+} concentrations. (Scale bar, 20 μm.) (*O*) Statistical analysis of fluorescence intensity at different culture times (D, day) shows a 3-fold increment of intracellular Ca^{2+} in *rd1* cells after 11 days in culture. Treatment with a calcium channel blocker, *cis*-diltiazem, prevents Ca^{2+} increase (D11dtz). Fluorescence intensity was reported as the mean amplitude of 20 different transversal layers of 20 cells. (*P*) Colabeling of *rd1*-differentiated retinal cells with TUNEL (red) and a substrate measuring calpain activity (blue). Arrows indicate cells with active calpains but that are not yet TUNEL-positive. (*Q*) Percentage of positive cells at 9, 10, and 11 days of culture: high Ca^{2+} (yellow), calpain activation (light blue), nuclear AIF (dark blue), nuclear caspase-12 (red), and TUNEL (green). (*R*) Quantitative real-time PCR shows increased *Caspase-12* mRNA levels in *rd1* cells.

and disrupts Ca^{2+} homeostasis (25), we observed cotranslocation of AIF and caspase-12 inside apoptotic nuclei (Fig. 7, which is published as supporting information on the PNAS web site). These data confirmed a direct correlation of intracellular Ca^{2+} concentration and translocation of apoptotic factors inside the nuclei.

We tracked the sequence of events during photoreceptor apoptosis. We found that, at 10 days of culture, the percentage of cells with high Ca^{2+} (Fig. 3 *N* and *Q*) is similar to cells activating calpain (Fig. 3 *P* and *Q*) and higher than $TUNEL^+$, nuclear AIF^+, and $caspase\text{-}12^+$ cells. We also detected cells in which calpains were activated but chromatin was not yet fragmented (Fig. 3*P*). At 9 and 10 days of differentiating culture, we observed a low percentage of cells in which AIF and caspase-12 have a nuclear localization but that are not yet labeled with TUNEL. Up-regulation of *Caspase-12* mRNA in *rd1* cells was also detected (Fig. 3*R*), as reported in motor-neuron degeneration (12).

All together, our data show that increase of intracellular Ca^{2+} in differentiated rods is directly correlated to calpain activation and, subsequently, to translocation of AIF and caspase-12 to nuclei. Furthermore, lack of cytochrome *c* release from mitochondria confirmed that translocations of AIF and caspase-12 are independent of executor caspase activation.

Roles of AIF and Caspase-12 During the Degenerative Process. To address the interaction between AIF and caspase-12 in degenerating photoreceptors, we used RNAi to knock down either AIF or caspase-12 in *in vitro*-differentiated *rd1* photoreceptors. Short hairpin (sh)RNAs showed high efficiency to knock down AIF (Fig. 4 *A*, *D*, and *O*) and caspase-12 (Fig. 4 *H*, *K*, and *P*). To rule out

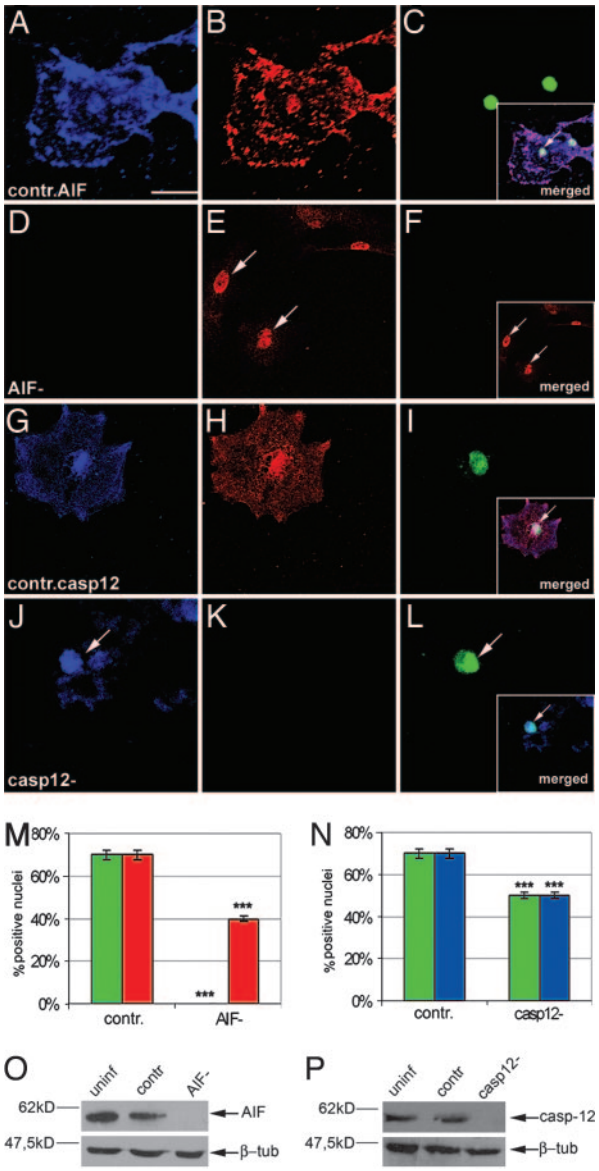

Fig. 4. Apoptosis in *rd1 in vitro*-differentiated photoreceptors in the absence of either AIF or caspase-12. Retinal cells from *rd1* mice were infected with retroviruses carrying AIF control shRNA (*A–C*, contr.AIF$^-$), AIF shRNA (*D–F*, AIF$^-$), caspase-12 control shRNA (*G–I*, contr.casp-12$^-$), and caspase-12 shRNA (*J–L*, casp-12$^-$). Cells were triple stained with anti-AIF (blue), anti-caspase-12 (red), and TUNEL (green). Merged images are shown in *Insets* of *C*, *F*, *I*, and *L* (merged). (Scale bar, 10 μm.) (*M* and *N*) Percentage of TUNEL- (green bars), caspase-12- (red bars), and AIF- (blue bars) positive nuclei of retinal stem cells infected with shRNA retroviruses targeting AIF (*M*) or caspase-12 (*N*). The values represent the average of nine different experiments. $P < 0.001$. (*O* and *P*) Western blotting of total proteins purified from RNAi experiments targeting either AIF (*O*) or caspase-12 (*P*) show complete down-regulation of these proteins. Uninf, samples of cells not treated with any shRNA retrovirus; cont, control shRNA. Western blots were normalized with the β-tubulin (β-tub).

nonspecific effects of shRNAs, we designed a second shRNA for each gene and confirmed that off-target effects are not responsible for the observed phenotype. Furthermore, down-regulation of AIF did not affect subcellular localization of mitochondrial cytochrome *c*, and down-regulation of caspase-12 did not affect ER marker ERAB (Fig. 8, which is published as supporting information on the PNAS web site). Mutagenized shRNAs were used as controls (Fig. 4 *A–C* and *G–I*). When AIF was down-regulated, a reduced number of photoreceptors showed caspase-12 translocation to the nucleus (Fig. 4 *E*, arrows, and *M*), and no chromatin fragmentation could be detected by TUNEL staining (Fig. 4 *F* and *M*). Conversely, down-regulation of caspase-12 only slightly reduced the percentage of dying cells (30% reduction, Fig. 4*N*), and all cells undergoing apoptosis showed nuclear localization of AIF, suggesting a primary role of AIF in this apoptotic event (Fig. 4 *J–N*). AIF is therefore necessary to activate apoptosis, whereas translocation of caspase-12 is not sufficient to induce apoptosis in photoreceptor cells. Similar results were obtained with the second shRNAs targeting either AIF or caspase-12 (Fig. 8).

Knockdown experiments suggested that mitochondrial and ER pathways are activated independently; however, the two pathways interact by reinforcing each other, as indicated by the reduced number of photoreceptors with nuclear localization of caspase-12 in AIF$^-$ cells or AIF in casp-12$^-$ cells.

Calcium Channel Blocker Interferes with AIF and Caspase-12 Activation. To confirm that changes in Ca^{2+} homeostasis cause AIF and caspase-12 relocalization, we treated *rd1* pups with the calcium channel blocker *cis*-diltiazem, a drug reported to be able to slow retinal degeneration in *rd1* mice (26). A significant decrease of apoptotic nuclei was found at P11. However, TUNEL-positive cells were still detectable, and histological analysis of *cis*-diltiazem-treated *rd1* retinas defined advanced degeneration at P21 (Fig. 5*I* and data not shown). No nuclear translocation of either AIF or caspase-12 was detectable by triple staining of *cis*-diltiazem-treated *rd1* retinas (Fig. 5 *A–D*). We also detected a strong decrease of activated AIF and caspase-12 fragments in the nuclear fraction of retinas treated with the calcium blocker (Fig. 5*K*). *cis*-diltiazem was also able to reduce apoptosis *in vitro* (Fig. 5*J*) and prevented AIF and caspase-12 translocation to the nucleus (data not shown). These data implied that changes in Ca^{2+} concentration are strictly linked to activation of multiple apoptotic pathways in *rd1* retinas.

Calpain Inhibitors Interfere with AIF and Caspase-12 Activation and Block Apoptosis in the *rd1* Retina. Cleavage and release of AIF from the mitochondria is mediated by calpain I (18), whereas caspase-12 is processed by calpain II (10). Based on this evidence, we reasoned that by blocking both calpain activities, we might prevent AIF and caspase-12 activation and, consequently, apoptosis. We intravitreously injected *rd1* eyes with either calpain inhibitors I (ALLN) or II (ALLM) or a mixture of both. We injected calpain inhibitors at concentrations reported for the eye (7). After treatment with both calpain inhibitors, we were unable to detect apoptotic cells in the *rd1* retina or in *in vitro*-differentiated photoreceptors (Fig. 5 *G–I*). *In vivo* treatments with ALLM or ALLN were not as effective as with the two inhibitors together (Fig. 5*I*). We never detected AIF and caspase-12 inside photoreceptor nuclei treated with ALLN and ALLM (Fig. 5 *E–H*). Western blot analysis confirmed that treatment with ALLN and ALLM was inhibiting AIF and caspase-12 activation (Fig. 5*K*). On the contrary, *in vivo* and *in vitro* treatment of *rd1* photoreceptors with pancaspase inhibitor zVAD.fmk had only a minor effect in preventing apoptosis and did not prevent nuclear localization of AIF and caspase-12 (Fig. 5 *I* and *J* and *L* and *M*).

Discussion

During the last 20 years, the molecular causes of RP were unraveled, and apoptosis was identified as the common mechanism causing photoreceptor demise in this genetically heterogeneous disease. Nevertheless, important questions on programmed cell death remained unsolved, and little is known about the apoptotic molecules activated in retinal degeneration. Here, we molecularly characterized apoptosis in photoreceptors with *Pde6b* gene inactivation. We report concomitant translocation to the nucleus of a mitochondrial protein, AIF, and of a caspase normally localized to the ER.

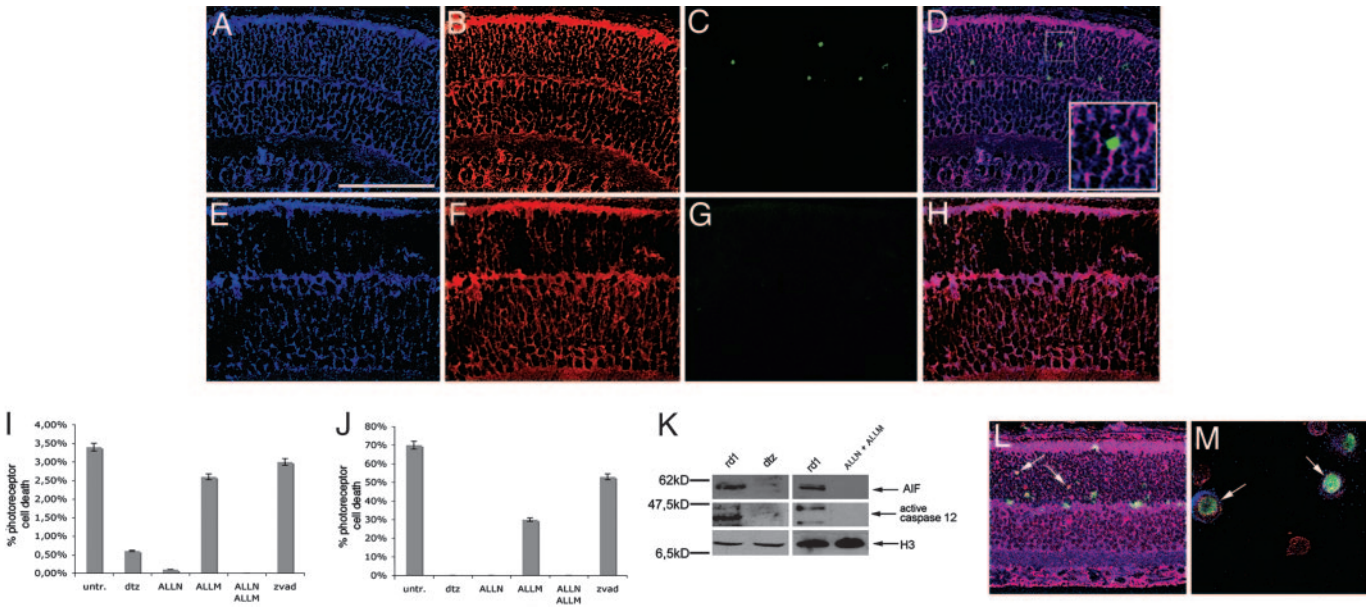

Fig. 5. *In vivo* and *in vitro* treatment of *rd1* photoreceptors with *cis*-diltiazem and calpain inhibitors. (*A–D*) P11 *rd1* retina treated with *cis*-diltiazem and triple stained with anti-AIF (blue), anti-caspase-12 (red), and TUNEL (green). The merged image is shown in *D*. (*D Inset*) Enlargement of the selected area is shown. (Scale bar, 100 μm.) (*E–H*) P11 *rd1* retina treated with ALLN and ALLM calpain inhibitors. Sections were triple stained with anti-AIF (blue), anti-caspase-12 (red), and TUNEL (green). The merged image is shown in *H*. (*I* and *J*) Counts of apoptotic photoreceptors in *rd1* retinas (*I*) and in *in vitro*-differentiated apoptotic photoreceptors (*J*) either untreated (untr.) or treated with *cis*-diltiazem (dtz), ALLN (ALLN), ALLM (ALLM), ALLN+ALLM (ALLN ALLM), or zVAD.fmk (zvad). The *y* axis in *I* represents mean values counted in six sections of six different mice. The *y* axis in *J* represents mean values counted in six different experiments. (*K*) Western blot analysis of nuclear-enriched lysates purified from P11 *rd1* (rd1), *rd1 cis*-diltiazem treated (dtz) and *rd1*-calpain inhibitor-treated (ALLN+ALLM) retinas. Western blots were normalized with the nuclear marker acetyl-histone H3 (H3). (*L*) retina section from a P11 *rd1* mouse intravitreally injected with zVAD.fmk and triple stained with TUNEL (green), anti-AIF antibodies (blue), and anti-caspase-12 antibodies (red). Arrows indicate cotranslocation of AIF and caspase-12 inside photoreceptor nuclei. (*M*) *In vitro*-differentiated *rd1* photoreceptors treated with zVAD.fmk (zvad) and stained with TUNEL (green), anti-AIF antibodies (blue), and anti-caspase-12 antibodies (red). Arrows indicate cotranslocation of AIF and caspase-12 inside apoptotic photoreceptor nuclei.

We observed that cotranslocation of AIF and caspase-12 in apoptotic photoreceptor nuclei follows increase of intracellular Ca^{2+} and calpain activation. The strict correlation with changes in Ca^{2+} homeostasis was confirmed by treatment with the calcium-channel blocker *cis*-diltiazem, which was able to reduce intracellular Ca^{2+}, interfere with translocation to the nucleus of both factors, and reduce apoptosis. We still cannot explain why the drug was unable to abolish apoptosis *in vivo*. The efficacy of *cis*-diltiazem in protecting against photoreceptor apoptosis is still controversial. Some studies provided evidence of photoreceptor rescue (26). In contrast, other studies did not detect beneficial effects in this same model (27) or in a canine model (28). By calculating the number of apoptotic cells during *cis*-diltiazem treatment, we detected some beneficial effect at early stages during the degenerative process; however, this drug was unable to completely block apoptosis, and the retina eventually underwent complete degeneration. We think that the *in vivo* treatment of mice with *cis*-diltiazem does not allow all photoreceptors to be exposed to the proper concentration, whereas the *in vitro* studies allow a more homogeneous exposure to the drug. Secondly, *cis*-diltiazem blocks all calcium channels and therefore deeply changes photoreceptor metabolism and interactions with adjacent cells, and this change may hamper the positive effects of the drug.

More interestingly, RNAi experiments implied that the two apoptotic factors are independently activated but partially affect each other. In fact, translocation to the nucleus of either AIF or caspase-12 can still be detected in the absence of the other factor, but in a low percentage of cells. We also demonstrated that AIF plays a crucial role in the apoptotic event of photoreceptor cells, whereas caspase-12 has a marginal role. In fact, down-regulation of this protein only partially rescues cells from apoptosis. Unfortunately, *in vivo* down-regulation of AIF cannot be tested because it causes degeneration of cerebellar and retinal neurons in the Harlequin mouse (29). It is therefore important to develop a system able to prevent AIF translocation to the nucleus without impairing its important physiological functions in the mitochondria. Our *in vivo* positive results with calpain-inhibitor treatments are the first attempt toward this aim and demonstrate the effectiveness of these drugs in blocking AIF activation. Our results are in line with the study showing a beneficial effect of different calpain inhibitors in retinal explant cultures (8), whereas it is not in agreement with a report showing no effect on photoreceptor degeneration by treatment with the calpain inhibitor ALLN (5). This discrepancy may be due to differences in the technical approaches used: Doonan *et al*. used retinal explants, whereas we treated mice *in vivo*; second, we used a mixture of two calpain inhibitors with high concentrations that are not toxic for the retina *in vivo*.

How can we explain the 20% of photoreceptors in which we did not observe AIF and caspase-12 translocation to the nucleus? We cannot exclude that our *in situ* detection of AIF and caspase-12 fails to detect low amounts of these factors in some apoptotic nuclei. In fact, photoreceptors in an advanced apoptotic status may degrade intracellular proteins like AIF and caspase-12, whereas the nucleus can still be labeled by TUNEL. We can also postulate that a third apoptotic pathway is activated in different photoreceptors, either independently or as a consequence of cell death in the surrounding cells. The minor effect of pancaspase inhibitor in reducing apoptosis *in vivo* and *in vitro* but not in preventing AIF and caspase-12 nuclear translocation may support this hypothesis; however, it may also imply a partial, but not key, function of effector caspases, as suggested (23).

In conclusion, the option of exploiting apoptosis as a therapeutic target is complex. Nevertheless, the molecular understanding of the different apoptotic factors activated during degeneration and the

identification of common activators are the first steps toward this goal. Our studies report an *in vivo* molecular characterization of apoptosis in *rd1* mice and identify AIF and caspase-12 as the apoptotic factors triggering photoreceptor cell demise. Coactivation of these two pathways may be involved in other forms of neuronal degenerations in which either AIF or caspase-12 were shown to be required (9, 11, 12, 30). We had demonstrated that the mitochondrial and ER pathways are engaged together in ER stress-activated apoptosis (25). Further studies will be necessary to define whether this mechanism is a common pathway triggered also in dominant forms of retinal degeneration caused by ER retention of mutant protein. Importantly, we defined that common activators, such as calpains, act on both mitochondrial and ER factors during the degenerative process. The efficacy of ALLN and ALLM in interfering with apoptosis and relocalization of AIF and caspase-12 opens new perspectives for designing therapeutic approaches to rescue photoreceptor cell death.

Materials and Methods

Mice and Treatments. All procedures on mice were performed in accordance with institutional guidelines for animal research. C3H/HeN (*rd1*) and CBA mice (genetic background of C3H/HeNCrl) were purchased from Charles River Italia (Calco, Italy). For intravitreal administration, calpain inhibitor I (ALLN, 10 nmol per eye, ≈1 mM final concentration) and II (ALLM, 2 nmol per eye, ≈200 μM final concentration) or zVAD.fmk (25 ng per eye) were delivered intravitreusly by a transscleral transchoroidal approach at P10. Control eyes received vehicle only (DMSO). I.p. injections of D-*cis*-diltiazem in *rd1* mice were performed as reported, starting at P7 (26). Treated mice were analyzed at P11. Adult C57BL/6 mice were i.p.-injected with a 70 mg/kg single dose of *N*-methyl-*N*-nitrosourea. Animals were killed 24 h after treatment.

Retinal Cell Culture Preparation and Differentiation. Retinal stem cells were isolated from adult mice and cultured as described (24). Retinal neurospheres were allowed to differentiate with 1% FBS on a substrate of laminin (2.5 μg/ml) and polyD-lysine (20 μg/ml). Seventy percent of photoreceptor differentiation was obtained by treatment with 500 nM retinoic acid for 11 days. Wt and *rd1*-differentiated retinal cells were treated with ALLN (25 μM), ALLM (5 μM), zVAD.fmk (50 μM), and D-*cis*-diltiazem (5 mM) for 12 h before analysis.

DNA Nick-End Labeling by the TUNEL Method and Immunofluorescence. Apoptotic nuclei were detected by TdT-mediated dUTP terminal nick-end labeling kit (TUNEL). Calpain activity was revealed as reported (5, 8). The primary antibodies used were: anti-AIF, anti-caspase-12, anti-rhodopsin (Ret-P1), anti-α subunit of protein kinase c (Pkcα), anti-Syntaxin, anti-Calbindin, all from Sigma (St. Louis, MO), anti-Pde6b from Abcam (Cambridge, U.K.), and anti-Cnga (31, 32).

Quantitative RT-PCR. The Real-time PCR was performed by using, as primers for *Casp-12* gene, casp-F: 5′-TTGCTTTCAAATCTTCTACCCCA and casp-R: 5′-GGAAATGAAGAGGGAACCAGTCTT and for *S26* reference gene, S26F: 5′-AAGTTTGTCATTCGGAACATT and S26R: 5′-GATCGATTCCTAACAACCTTG.

Calcium Ion Concentration Measurement. Fluo-4, AM (Molecular Probes, Eugene, OR) was loaded into differentiated photoreceptor cells for 30 min at 37°C in Ca^{2+}-free medium. Cells were excited by using a 488-nm laser beam and analyzed with a Laser Confocal Microscope System (Leica, Wetzlar, Germany). Twenty sequential layers of each cell were photographed. Images were then analyzed with the Leica confocal software (LCS). The fluorescence average intensity (mean amplitude) of each area was measured.

Western Blotting Analysis. Retinas were lysed as described (25). The antibodies used for Western blotting were anti-AIF (Oncogene, Cambridge, MA) and anti-caspase-12 (Cell Signaling Technology, Beverly, MA).

RNAi. Target sequences for *caspase-12* mRNA were 5′-AAUGAUGAGGAUGAUGGACCU and 5′-AACCCAAGAUUCUCAUCAUGC. Control hairpin RNAi template oligonucleotides were generated by mutagenizing three nucleotides (in bold) in the targeting sequence: AATG**CC**G**C**GGATGATGGACCT. Targeting sequences for AIF were 5′-UUGUUCCAGCAAUGGCGUG and 5′-CUUGUUCCAGCAAUGGCGU. As control, we mutated three nucleotides (in bold) in the targeting sequence: TT**C**TTC**T**AG**A**AATGGCGTG. Sense and antisense oligonucleotides were annealed to form a hairpin siRNA template insert and were cloned into the pSUPER Maloney-derived retroviral vector. Retinal cell cultures were infected at day 4 of differentiation with retroviruses obtained by transient transfection in HEK293T cells and diluted 1:100. Cells were analyzed 6 days later.

We thank R. S. Molday (University of British Columbia, Vancouver, BC, Canada) for generously providing 1D1 anti-Cnga antibody; E. Rugarli, P. Ekström, and F. Paquet-Durand for discussion on the data; and S. Arbucci for confocal microscopy. This work was supported by research grants from Fondazione Telethon and European Vision Institute-GENORET (LSHG-CT-2005-512036) from the European Community (to V.M.).

1. McLaughlin ME, Sandberg MA, Berson EL, Dryja TP (1993) *Nat Genet* 4:130–134.
2. Bowes C, Li T, Danciger M, Baxter LC, Applebury ML, Farber DB (1990) *Nature* 347:677–680.
3. Farber DB, Lolley RN (1974) *Science* 186:449–451.
4. Lolley RN, Farber DB, Rayborn ME, Hollyfield JG (1977) *Science* 196:664–666.
5. Doonan F, Donovan M, Cotter TG (2005) *Invest Ophthalmol Vis Sci* 46:3530–3538.
6. Wang KK (2000) *Trends Neurosci* 23:20–26.
7. Chiu K, Lam TT, Ying Li WW, Caprioli J, Kwong Kwong JM (2005) *Brain Res* 1046:207–215.
8. Paquet-Durand F, Azadi S, Hauck SM, Ueffing M, van Veen T, Ekstrom P (2006) *J Neurochem* 96:802–814.
9. Nakagawa T, Zhu H, Morishima N, Li E, Xu J, Yankner BA, Yuan J (2000) *Nature* 403:98–103.
10. Nakagawa T, Yuan J (2000) *J Cell Biol* 150:887–894.
11. Hetz C, Russelakis-Carneiro M, Maundrell K, Castilla J, Soto C (2003) *EMBO J* 22:5435–5445.
12. Wootz H, Hansson I, Korhonen L, Napankangas U, Lindholm D (2004) *Biochem Biophys Res Commun* 322:281–286.
13. Fujita E, Kouroku Y, Jimbo A, Isoai A, Maruyama K, Momoi T (2002) *Cell Death Differ* 9:1108–1114.
14. Susin SA, Lorenzo HK, Zamzami N, Marzo I, Snow BE, Brothers GM, Mangion J, Jacotot E, Costantini P, Loeffler M, *et al.* (1999) *Nature* 397:441–446.
15. Chu CT, Zhu JH, Cao G, Signore A, Wang S, Chen J (2005) *J Neurochem* 94:1685–1695.
16. Hisatomi T, Sakamoto T, Murata T, Yamanaka I, Oshima Y, Hata Y, Ishibashi T, Inomata H, Susin SA, Kroemer G (2001) *Am J Pathol* 158:1271–1278.
17. Wang H, Yu SW, Koh DW, Lew J, Coombs C, Bowers W, Federoff HJ, Poirier GG, Dawson TM, Dawson VL (2004) *J Neurosci* 24:10963–10973.
18. Polster BM, Basanez G, Etxebarria A, Hardwick JM, Nicholls DG (2005) *J Biol Chem* 280:6447–6454.
19. Cande C, Vahsen N, Garrido C, Kroemer G (2004) *Cell Death Differ* 11:591–595.
20. Hauck SM, Ekström P, Ahuja-Jensen O, Suppmann S, Paquet-Durand F, van Veen T, Ueffing M (2006) *Mol Cell Proteomics* 5:324–336.
21. Carter-Dawson LD, LaVail MM, Sidman RL (1978) *Invest Ophthalmol Vis Sci* 17:489–498.
22. Doonan F, Donovan M, Cotter TG (2003) *J Neurosci* 23:5723–5731.
23. Zeiss CJ, Neal J, Johnson EA (2004) *Invest Ophthalmol Vis Sci* 45:964–970.
24. Tropepe V, Coles BL, Chiasson BJ, Horsford DJ, Elia AJ, McInnes RR, van der Kooy D (2000) *Science* 287:2032–2036.
25. Sanges D, Marigo V (2006) *Apoptosis* 11:1629–1641.
26. Frasson M, Sahel JA, Fabre M, Simonutti M, Dreyfus H, Picaud S (1999) *Nat Med* 5:1183–1187.
27. Pawlyk BS, Li T, Scimeca MS, Sandberg MA, Berson EL (2002) *Invest Ophthalmol Vis Sci* 43:1912–1915.
28. Pearce-Kelling SE, Aleman TS, Nickle A, Laties AM, Aguirre GD, Jacobson SG, Acland GM (2001) *Mol Vis* 7:42–47.
29. Klein JA, Longo-Guess CM, Rossmann MP, Seburn KL, Hurd RE, Frankel WN, Bronson RT, Ackerman SL (2002) *Nature* 419:367–374.
30. Cande C, Cecconi F, Dessen P, Kroemer G (2002) *J Cell Sci* 115:4727–4734.
31. Cook NJ, Molday LL, Reid D, Kaupp UB, Molday RS (1989) *J Biol Chem* 264:6996–6999.
32. Wassle H, Grunert U, Cook NJ, Molday RS (1992) *Neurosci Lett* 134:199–202.